

# One-dimensional hard x-ray field retrieval using a moveable structure

Manuel Guizar-Sicairos<sup>\*,1,2</sup>, Kenneth Evans-Lutterodt<sup>3</sup>, Abdel F. Isakovic<sup>3,5</sup>, Aaron Stein<sup>3</sup>, John B. Warren<sup>3</sup>, Alec R. Sandy<sup>4</sup>, Suresh Narayanan<sup>4</sup> and James R. Fienup<sup>1</sup>

<sup>1</sup>The Institute of Optics, University of Rochester, Rochester, New York, 14627, USA

<sup>2</sup>Current address: Paul Scherrer Institut, CH-5232 Villigen PSI, Switzerland

<sup>3</sup>Brookhaven National Laboratory, Upton, New York, 11973, USA

<sup>4</sup>Argonne National Laboratory, Argonne, Illinois, 60439, USA

<sup>5</sup>KUSTAR, P.O. Box 127788, Abu Dhabi, United Arab Emirates

[\\*manuel.guizar-sicairos@psi.ch](mailto:*manuel.guizar-sicairos@psi.ch)

**Abstract:** We present a technique that allows measuring the field of an x-ray line focus using far-field intensity measurements only. One-dimensional phase retrieval with transverse translation diversity is used to recover a hard x-ray beam focused by a compound kinoform lens. The reconstruction is found to be in good agreement with independent knife-edge scan measurements taken at separated planes. The approach avoids the need for measuring the beam profile at focus and allows narrower beams to be measured than the traditional knife-edge scan.

© 2010 Optical Society of America

**OCIS codes:** (100.5070) Phase retrieval; (140.3295) Laser beam characterization; (340.7480) X-rays, soft x-rays, extreme ultraviolet (EUV); (110.7440) X-ray imaging.

---

## References and links

1. H. Mimura, S. Handa, T. Kimura, H. Yumoto, D. Yamakawa, H. Yokoyama, S. Matsuyama, K. Inagaki, K. Yamamura, Y. Sano, K. Tamasaku, Y. Nishino, M. Yabashi, T. Ishikawa and K. Yamauchi, "Breaking the 10 nm barrier in hard-X-ray focusing," *Nat. Physics* **6**, 122–125 (2010).
2. H. C. Kang, J. Maser, G. B. Stephenson, C. Liu, R. Conley, A. T. Macrander and S. Vogt, "Nanometer linear focusing of hard x rays by a multilayer Laue lens," *Phys. Rev. Lett.* **96**, 127401 (2006).
3. K. Evans-Lutterodt, A. Stein, J. M. Ablett, N. Bozovic, A. Taylor and D. M. Tennant, "Using compound kinoform hard-x-ray lenses to exceed the critical angle limit," *Phys. Rev. Lett.* **99**, 134801 (2007).
4. H. C. Kang, H. Yan, R. P. Winarski, M. V. Holt, J. Maser, C. Liu, R. Conley, S. Vogt, A. T. Macrander and G. B. Stephenson, "Focusing of hard x-rays to 16 nanometers with a multilayer Laue lens," *Appl. Phys. Lett.* **92**, 221114 (2008).
5. A. Stein, K. Evans-Lutterodt, N. Bozovic and A. Taylor, "Fabrication of silicon kinoform lenses for hard x-ray focusing by electron beam lithography and deep reactive ion etching," *J. Vac. Sci. Technol. B* **26**, 122–127 (2008).
6. T. Kimura, S. Handa, H. Mimura, H. Yumoto, D. Yamakawa, S. Matsuyama, K. Inagaki, Y. Sano, K. Tamasaku, Y. Nishino, M. Yabashi, T. Ishikawa and K. Yamauchi, "Wavefront Control System for Phase Compensation in Hard X-ray Optics," *Jpn. J. Appl. Phys.* **48**, 072503 (2009).
7. H. Mimura, H. Yumoto, S. Matsuyama, S. Handa, T. Kimura, Y. Sano, M. Yabashi, Y. Nishino, K. Tamasaku, T. Ishikawa and K. Yamauchi, "Direct determination of the wave field of an x-ray nanobeam," *Phys. Rev. A* **77**, 015812 (2008).
8. H. M. Quiney, A. G. Peele, Z. Cai, D. Paterson and K. A. Nugent, "Diffraction imaging of highly focused x-ray fields," *Nat. Physics* **2**, 101–104 (2006).
9. M. Guizar-Sicairos and J. R. Fienup, "Measurement of coherent x-ray focused beams by phase retrieval with transverse translation diversity," *Opt. Express* **17**, 2670–2685 (2009).
10. H. M. L. Faulkner and J. M. Rodenburg, "Movable aperture lensless transmission microscopy: a novel phase retrieval algorithm," *Phys. Rev. Lett.* **93**, 023903 (2004).

11. M. Guizar-Sicairos and J. R. Fienup, "Phase retrieval with transverse translation diversity: a nonlinear optimization approach," *Opt. Express* **16**, 7264–7278 (2008).
12. P. Thibault, M. Dierolf, A. Menzel, O. Bunk, C. David and F. Pfeiffer, "High-resolution scanning x-ray diffraction microscopy," *Science* **321**, 379–382 (2008).
13. A. M. Maiden and J. M. Rodenburg, "An improved ptychographical phase retrieval algorithm for diffractive imaging," *Ultramicroscopy* **109**, 1256–1262 (2009).
14. G. R. Brady, M. Guizar-Sicairos and J. R. Fienup, "Optical wavefront measurement using phase retrieval with transverse translation diversity," *Opt. Express* **17**, 624–639 (2009).
15. A. F. Isakovic, K. Evans-Lutterodt, D. Elliott, A. Stein, and J. B. Warren, "Cyclic, cryogenic, highly anisotropic plasma etching of silicon using SF<sub>6</sub>/O<sub>2</sub>," *J. Vac. Sci. Technol. A* **26**, 1182–1187 (2008).
16. See for example, [T. R. Crimmins and J. R. Fienup, "Ambiguity of phase retrieval for functions with disconnected support," *J. Opt. Soc. Am.* **71**, 1026–1028 (1981)], and references within.
17. B. C. McCallum and J. M. Rodenburg, "Two-dimensional demonstration of Wigner phase-retrieval microscopy in the STEM configuration," *Ultramicroscopy* **45**, 371–380 (1992).
18. S. H. Nawab, T. F. Quatieri and J. S. Lim, "Signal reconstruction from short-time Fourier transform magnitude," *IEEE Trans. Acoust., Speech, Signal Process.* **31**, 986–998 (1983).
19. O. Bunk, M. Dierolf, S. Kynde, I. Johnson, O. Marti and F. Pfeiffer, "Influence of the overlap parameter on the convergence of the ptychographical iterative engine," *Ultramicroscopy* **108**, 481–487 (2008).
20. C. M. Kewish, P. Thibault, M. Dierolf, O. Bunk, A. Menzel, J. Vila-Comamala, K. Jefimovs and F. Pfeiffer, "Ptychographic characterization of the wavefield in the focus of reflective hard X-ray optics," *Ultramicroscopy* **110**, 325–329 (2010).
21. A. Schropp, P. Boye, J. M. Feldkamp, R. Hoppe, J. Patommel, D. Samberg, S. Stephan, K. Giewekemeyer, R. N. Wilke, T. Salditt, J. Gulden, A. P. Mancuso, I. A. Vartanyants, E. Weckert, S. Schöder, M. Burghammer and C. G. Schroer, "Hard x-ray nanobeam characterization by coherent diffraction microscopy," *Appl. Phys. Lett.* **96**, 091102 (2010).

## 1. Introduction

Producing hard x-ray spot sizes of 1 nanometer or below, in combination with the penetrating nature of hard x-ray photons, will enable structural and spectroscopic study of matter *in-situ* and in buried structures with unprecedented spatial resolution [1]. Diffraction with a focused beam of hard x-ray photons provides spatially resolved sensitivity to crystallographic phase, strain, and grain orientation. Additionally, x-ray spectroscopic and fluorescence measurements with these focused x-ray beams will provide spatially resolved maps of elemental composition and chemical state.

There are ongoing research efforts dedicated towards reducing the size of hard x-ray focused spots in order to bring the spatial resolution closer to the theoretical limits. Due to the technical challenges in fabricating hard x-ray optics that produce small two-dimensional spots, it is anticipated that the smallest focused spots will be produced by one-dimensional lenses that individually produce a one-dimensional line focus [1–6]. A crossed pair of these one-dimensional optics can produce a two-dimensional spot, as in the familiar Kirkpatrick-Baez mirror arrangement.

A widely accepted at-wavelength characterization technique is to measure the spot size by scanning a thin metal slab through the beam, while monitoring the emitted fluorescence. This method can be technically very challenging and time consuming, even with current state-of-the-art focused spots of diameter around 10 nanometers. These difficulties arise because the transverse size or resolution of the slab has to be significantly smaller than the spot size ( $\lambda/NA$ ), and the longitudinal size has to be smaller than the depth of field ( $\lambda/NA^2$ ), where  $\lambda$  is the illumination wavelength and NA is the numerical aperture of the x-ray optics. This fact implies that the effective cross-section of material in the slab decreases as  $\lambda^2/NA^3$ , resulting in a rapidly decreasing signal-to-noise ratio for higher numerical apertures. Ultimately, typical interatomic distances ( $\sim 0.3$  nm) will become a limitation for this approach. In an extreme case one can envision measuring a 1 nm beam ( $\lambda = 0.1$  nm and NA = 0.1, for example) by fabricating a slab of a single layer of atoms in the transverse direction with a longitudinal dimension of about 10 nm, clearly very technically challenging. These measurements are further complicated by

stringent requirements on alignment, positioning accuracy and stability. Finally, an intensity profile can be used to determine whether the optic is performing as designed or not, but it provides limited diagnostic information about wavefront aberrations. Clearly alternative means of characterization would be helpful.

Phase retrieval methods provide an attractive alternative because they reconstruct complex-valued fields, which yield the specifics of the aberration, and have more potential as an *in situ*, at-wavelength diagnostic tool. We anticipate that these techniques will play an increasingly important role in coherent x-ray focused beam diagnostics. Successful examples of using phase retrieval for this task include the work of Mimura *et al.* [1, 7] which relies on an accurate high-resolution measurement of the beam intensity at focus, and Quiney *et al.* [8] which lacks diverse measurements that are desirable to improve algorithm convergence and robustness and that are especially important for the one-dimensional case.

In this paper we present an experimental demonstration of a one-dimensional phase retrieval technique that circumvents these limitations and allows recovery of a one-dimensional (line) focus [9], an important capability for testing the performance of individual cylindrical optics. We use one-dimensional phase retrieval with transverse translation diversity (TTD) to robustly reconstruct a coherent hard x-ray field focused by a single cylindrical lens. For this approach a structure is placed in the path of the beam and translated transversely to the direction of propagation, thus perturbing the incident beam. For each position of the translating structure, a different diffraction pattern is measured, and these measurements are fed into a phase retrieval algorithm to recover the x-ray field incident on the structure. The multiple diffraction patterns provide suitable diverse measurements that allow a robust solution of the phase retrieval problem, even in one dimension. Appendix A discusses how TTD alleviates the one-dimensional phase retrieval uniqueness problem. Using this technique, an intensity beam profile near focus is not necessary, the structure does not need to be within the depth of focus of the beam, and its transverse size and translations can be significantly larger than the desired resolution. These characteristics will become increasingly important as the size of the x-ray focused spots is reduced.

Phase retrieval with TTD was first introduced by Faulkner *et al.* for x-ray diffractive imaging [10]. Since then, reconstruction algorithms that are capable of refining the initial knowledge of the incident illumination [11–13] and sample translations [11] have been developed. More recently, the applicability of this technique to extend the range of phase retrieval for optical wavefront measurement was experimentally demonstrated [14].

## 2. Data measurement and reconstruction

For our experiment, we characterized the beam focused by a compound kinoform lens with  $f = 10$  cm focal length. The lens was fabricated [5, 15] by first depositing etch-resistant hard-mask layers of silicon dioxide (100 nm) and aluminum nitride (200 nm) on a standard 300 mm diameter silicon wafer. Next, exposures were made via electron beam lithography (EBL) with a 100 keV JEOL JBX9300-FS patterning tool. Interferometric registration of the stage ensures that the elements of the kinoform are placed with an accuracy better than 20 nm. The lens pattern was transferred to the aluminum nitride layer in a LAM 9600 reactive ion etcher. The oxide masking layer was then etched in an Applied Materials 5200 Centura reactive-ion etching (RIE) machine. The 90  $\mu\text{m}$  deep etch into silicon is a Bosch process and was performed with a Surface Technology Systems deep RIE (DRIE).

Figure 1 shows the arrangement of the experiment carried out at the ID8 beamline of Argonne National Laboratory Advance Photon Source (ANL-APS). The photon energy of the illumination beam was  $E = 12$  keV ( $\lambda \approx 0.1$  nm) with a photon energy bandwidth of  $\Delta E/E \approx 10^{-4}$ . For our experimental parameters this beam can be considered temporally coherent, which is

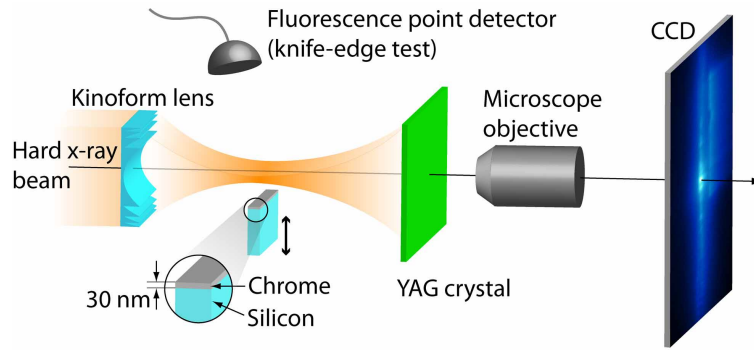


Fig. 1. Experimental arrangement allowing simultaneous measurement of the diffraction patterns for phase retrieval and a beam intensity profile for independent comparison.

an assumption of the phase retrieval algorithm. The x-ray beam was incident on the lens and brought to a horizontal line (1D) focus. The width of incident beam was  $200\ \mu\text{m}$  in the vertical direction, limited by the lens aperture. This aperture, along with the focal distance and the wavelength, determine the width of the diffraction-limited focus. In the horizontal direction the beam under-filled the lens and was  $20\ \mu\text{m}$  wide, as fixed by a slit upstream. Because the lens only focuses along the vertical direction, the horizontal length of the line focus is roughly equal to the horizontal slit width. Another important assumption of our phase retrieval algorithm is that the incident illumination is transversely coherent, which is reasonably satisfied on the  $20\ \mu\text{m} \times 200\ \mu\text{m}$  rectangular illumination window. Because the smallest focused spots can only be achieved under transversely coherent illumination, this assumption of the reconstruction algorithm is generally satisfied for x-ray nano-focusing applications.

A  $30\ \text{nm}$  layer of chrome deposited on a silicon wall was scanned through the beam, near focus, with  $40\ \text{nm}$  steps. A beam transverse intensity profile (fluorescent knife-edge) was obtained by measuring the fluorescent signal of the chrome slab using a Vortex detector about  $8\ \text{cm}$  away from the knife-edge in a near-perpendicular orientation to the direction of propagation of the x-ray beam.

For each position of the chrome and silicon structure, a diffraction intensity pattern was simultaneously measured. A fluorescent YAG crystal was placed  $20\ \text{cm}$  downstream from the structure, as shown in Fig. 1, and its fluorescent pattern was imaged to a CCD using a  $10\times$  microscope objective. The effective pixel size on the YAG crystal was  $0.67\ \mu\text{m}$ . Figure 2(a) shows one of the 51 measured diffraction patterns.

The moveable structure then serves a dual purpose: the silicon wall imparts a phase shift on the beam of about  $-2$  radians, allowing for suitably diverse intensity measurements that can be used by phase retrieval; and the detected fluorescence from the chrome slab provides a cut through the beam intensity we can use for an independent comparison.

Because of the spatial response of the YAG crystal, the diffraction patterns are blurred, which significantly affects the reconstructions. To reduce this effect we deconvolved each frame using a Wiener filter. The filter parameters were estimated by fitting the Fourier transform (FT) of the data to a model that included a power law for the signal spectrum, a flat noise power spectrum and an exponential point spread function (PSF) for the crystal response (*i.e.* a function that decays exponentially with radius). This mathematical form was inferred from inspection of the data. Improved results should be expected by careful characterization of the spatial response of the YAG crystal. Figure 2(b) shows the resulting diffraction pattern after deconvolution of the measurement in Fig. 2(a).

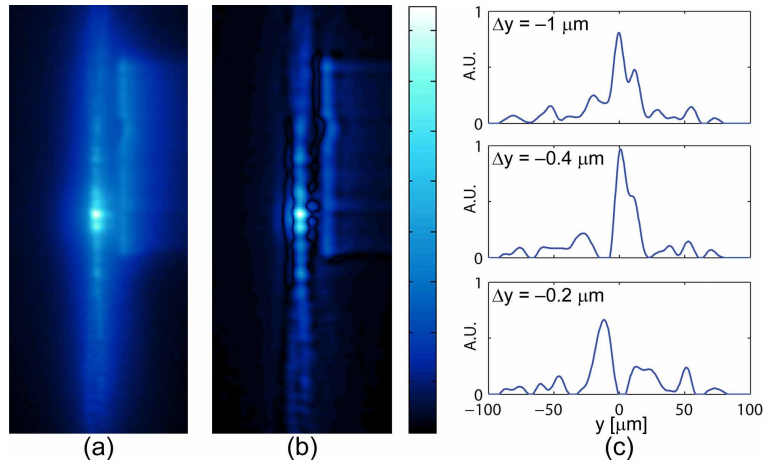


Fig. 2. (a) Intensity measurement for the moveable structure at  $\Delta y = -1 \mu\text{m}$ . (b) After deconvolution of (a). (c) Sample 1D intensity patterns used for phase retrieval, for different structure positions  $\Delta y$ , each obtained by integrating the deconvolved intensity measurements along the non-focusing (horizontal) direction.

The diffraction signal was extracted from each deconvolved frame and integrated along the horizontal direction, thus providing a set of one-dimensional intensity patterns, as shown in Fig. 2(c). Care was taken to exclude the stray light going around the lens that is evident to the right of the pattern in Fig. 2(b). These measurements, along with our *a priori* knowledge of the moveable structure and its translations, were fed to a nonlinear optimization algorithm for determining the x-ray field incident on the structure [11]. For the reconstructed field the sampling is 30 nm and the initial estimate of the beam for the phase retrieval algorithm was a Gaussian beam with a 100 nm waist and zero phase. Although in noisy numerical simulations we find the reconstruction to be very consistent under widely different starting guesses (*i.e.* uniform random numbers), for this case the reconstructions only converged with initial estimates that were close to the expected shape of the beam. We also tried a few Gaussian functions with radii in the range of 30 nm to 500 nm and observed they converged to similar results. This different behavior from the simulations may be attributable to the sub-optimal measurement conditions for the diffraction patterns (as more extensively discussed below) and possibly to other experimental uncertainties.

The numerical model for the structure was a complex-valued transmissivity obtained from the structure thickness ( $10 \mu\text{m}$ ) and known complex-valued indices of refraction of silicon and chrome. Although the silicon has a small absorption of about 2% in amplitude, it imparts a large phase shift to the beam and thus provides suitable diverse measurements.

Figure 3(a) compares the intensity of the reconstructed beam (after 350 iterations) to that obtained with the fluorescent knife-edge test, showing good agreement. Notice that both measurements have a similar beam width and that the beam is reconstructed with a left-right asymmetry that is consistent with the knife-edge intensity profile. The data from the fluorescent knife edge was not used by the phase retrieval algorithm.

Because phase retrieval recovers the complex-valued field, we can numerically propagate the reconstruction to any plane of interest. Figure 4(a) shows the numerical propagation of the reconstructed beam through focus. Notice that the plane of best focus is predicted to be upstream of the reconstruction plane.

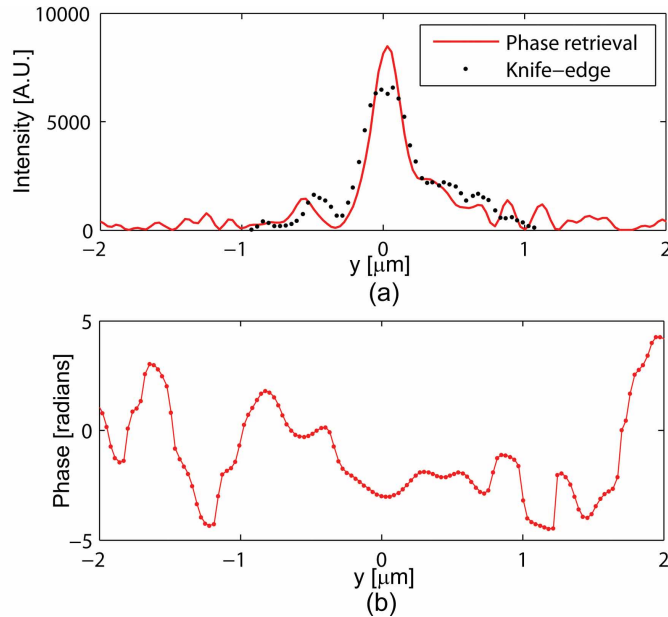


Fig. 3. (a) Comparison of phase retrieval reconstruction and the fluorescent knife-edge scanning. (b) Phase profile of the x-ray beam at the plane of the structure. The phase was originally computed modulo  $2\pi$  from the reconstructed field and unwrapped for easier visualization.

The reconstructed field was numerically propagated  $500 \mu\text{m}$  upstream, a plane where a second fluorescent knife-edge scan was performed. Figure 4(b) shows the comparison, which again exhibits good agreement. Both the knife-edge scan and the numerically propagated beam shown at this plane have a smaller waist and higher peak intensity, compared with the reconstruction plane.

For visual comparison, a common multiplicative factor was introduced for the phase retrieval intensity in Figs. 3(a) and 4(b).

Different sources of error in both measurements may be responsible for the differences shown in Figs. 3(a) and 4(b). The smaller peak on the knife-edge test may be attributable to saturation of the chrome fluorescence. On the other hand, the phase retrieval reconstruction may be affected by a nonlinear response from the YAG crystal and/or inaccurate estimation of the YAG crystal spatial response.

Using a direct CCD detection for the diffraction patterns may be advantageous for phase retrieval, since detection nonlinearities and spatial blur are reduced. This would, however, require a significantly more expensive detector due to x-ray detection dynamic range requirements. An alternative is to carefully characterize the crystal nonlinearity and spatial response for accurate *a posteriori* data compensation. Despite the additional burden of the characterization, this approach would enable the use of the technique with relatively inexpensive detectors. Further work is also needed to determine if there are moveable structure shapes that favor the reconstruction.

### 3. Summary

We have experimentally demonstrated the capability of phase retrieval with transverse translation diversity (TTD), to reconstruct a one-dimensional focused x-ray field from diffraction in-

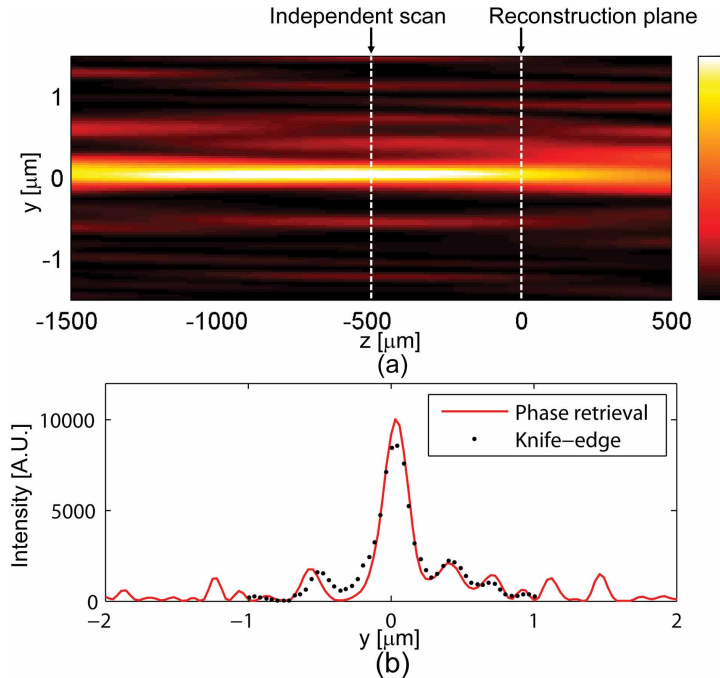


Fig. 4. (a) Numerical propagation of phase retrieval reconstruction through focus. The colorbar on the right is proportional to intensity. (b) Comparison of numerically propagated field to an independent fluorescent knife-edge scan performed 500  $\mu\text{m}$  upstream.

tensity measurements only. Through numerical propagation, the reconstruction was compared to fluorescent knife-edge scans taken at two planes 500 microns apart, and was found to be in good agreement. The numerically propagated beam revealed that the best focus position was upstream of the plane of the reconstruction, this fact was confirmed by the independent fluorescent knife-edge scans.

Phase retrieval with TTD is particularly well suited for characterizing small x-ray focused spots, because it avoids the need to precisely measure the beam intensity at focus, and its resolution is independent of the size and translations of the moveable structure. Alignment and stability are also relaxed since the structure need not be within the depth of focus of the beam. In principle, one can place a relatively large structure outside of the focal region and translate it in relatively large steps. From the reconstructions one can then deduce the spot size at any distance through numerical propagation.

Although we have demonstrated the technique with a compound kinoform lens, the algorithm requires no knowledge of the nature of the focusing optics. Thus, it can be straightforwardly applied to beams focused by mirrors or multilayer Laue lenses. Furthermore, because we solve a one-dimensional problem and we use a modest number of diffraction patterns, the computational time and memory requirements are significantly reduced, compared with the analogous two-dimensional problem.

Since the submission of this manuscript, two references that are very relevant to this work have come to our attention [20, 21]. In these papers the authors use phase retrieval with transverse translations to reconstruct a two-dimensional x-ray focused field.

## Appendix A: On the uniqueness of 1D phase retrieval with TTD

It is known that one-dimensional phase retrieval using a contiguous object support constraint and a Fourier transform (FT) intensity measurement is ambiguous. That is, one can find an enumerable set of non-equivalent solutions (that differ by more than a translation and global phase) that strictly satisfy both constraints [16]. However, in the framework of ptychography [17], the uniqueness of the solution to the phase retrieval problem with TTD is guaranteed through a direct computation method, if the illumination pattern is known. Although the formalism in Ref. [17] is applicable to the two- and one-dimensional cases alike, the resolution of this reconstruction procedure is ultimately limited by the translations of the illumination pattern, so that the resolution can be no finer than the translation step. Because phase retrieval with TTD is able to reconstruct with a resolution finer than the magnitude of the translations, for this case the uniqueness of the solution still remains to be explored.

To show how TTD can alleviate the uniqueness problem of one-dimensional phase retrieval for translations larger than the resolution, it is useful to recognize the close relation between this problem and that of reconstructing a signal from the magnitude of its short-time FT [18].

Consider the problem of reconstructing an object  $o(n)$  (where  $n$  is the sample number), from two intensity measurements,  $|F_0|^2$  and  $|F_1|^2$ , that correspond to the squared FTs of the fields  $f_0(n) = o(n)p(n)$  and  $f_1(n) = o(n)p(n-L)$ , respectively. Knowing the finite extent (support) of the illumination  $p(n)$  allows us to attempt recovery of  $f_0(n)$  from  $|F_0|^2$  using a support constraint. Suppose that  $p(n)$  has a support of  $N > L$  pixels. Assuming we found one of the solutions,  $\hat{f}_0(n)$ , that agrees with  $|F_0|^2$  and satisfies the support constraint, we can directly obtain an estimate of the object,  $\hat{o}(n) = \hat{f}_0(n)/p(n)$ , for the points within the support where  $p(n)$  is non-zero. This in turn provides an estimate for  $\hat{f}_1(n) = \hat{o}(n)p(n-L)$  for the  $N-L$  points of overlap of  $p(n)$  and  $p(n-L)$ .

Now consider the second measurement,  $|F_1|^2$ . Following the derivation in Ref. [18], it can be shown that, if  $L < N/2$  and  $p(n) \neq 0$  for all points inside its support, we can define a set of  $L$  independent linear equations to determine the remainder unknown coefficients of  $\hat{f}_1(n)$ . These equations use the estimated  $N-L$  points of  $\hat{f}_1(n)$  and  $L$  points of the autocorrelation  $f_1 \otimes f_1$ , which is given by the inverse FT of  $|F_1|^2$ . The requirement,  $L < N/2$ , assumes  $\hat{f}_1(L) \neq 0$ ; if this is not the case, an additional point of overlap is required to construct the set of equations. Although the analysis in Ref. [18] is for real valued signals, it can be straightforwardly extended to complex values.

The argument above has the following implication. Given the requirements outlined above, a solution  $\hat{f}_0(n)$  of  $|F_0|^2$  uniquely determines a solution  $\hat{f}_1(n)$  from only  $L$  points of  $f_1 \otimes f_1$ . The solution  $\hat{f}_0(n)$  should then predict the remainder  $N-L$  independent points of  $f_1 \otimes f_1$ . If a non-equivalent erroneous solution  $\hat{f}_0(n)$  for  $|F_0|^2$  was obtained and used to determine  $\hat{f}_1(n)$ , it is unlikely that  $\hat{f}_1(n)$  will be able to reproduce the  $N-L$  remainder points of the autocorrelation,  $f_1 \otimes f_1$ , which in turn means this estimate will not reproduce  $|F_1|^2$ . Thus, by requiring in this way that  $\hat{f}_0(n)$  be also consistent with  $|F_1|^2$ , most or all of the non-equivalent solutions from  $|F_0|^2$  are discarded. Through numerical simulations, with up to  $N = 21$  and  $L = 10$ , we observed that only one of the 1,048,576 solutions of  $|F_0|^2$  was able to reproduce  $|F_1|^2$  to within numerical precision.

Although the above statement does not prove the uniqueness of a solution, it exemplifies how, by requiring consistency with a second intensity measurement, TTD alleviates the one-dimensional phase retrieval uniqueness problem. Increasing the number of measurements further constrains the solution. Although the construction of the linear set of equations requires the translation step to be at most half of the extent of  $p(n)$ , we do not imply that this constraint is a requirement for TTD to improve upon phase retrieval with a support constraint. For the two-dimensional case, the benefit of TTD has been observed for translations larger than half of



the illumination diameter, although optimal convergence was observed for a linear overlap well above 50% [19]. The influence of the overlap parameter on the quality of the reconstructions still remains to be explored for the one-dimensional case.

### **Acknowledgements**

Use of the National Synchrotron Light Source (NSLS), the Center for Functional Nanomaterials and the NSLS-II project at Brookhaven National Laboratory was supported by the U. S. Department of Energy (DOE), Office of Basic Energy Sciences, under Contract No. DE-AC02-98CH10886. The use of ANL-APS was supported through the DOE contract DE-AC02-06CH11357. We thank C. C. Kao for financial support.